Sum rule for optical scattering rates

F. Marsiglio,[1] J. P. Carbotte,[2] and E. Schachinger[3]
[1]*Physics Department, University of Alberta, Edmonton, Alberta, Canada T6G 2J1*
[2]*Department of Physics and Astronomy, McMaster University, Hamilton, Ontario, Canada L8S 4M1*
[3]*Institut für Theoretische Physik, Technische Universität Graz, A-8010 Graz, Austria*
(Received 31 May 2001; published 7 December 2001)

An important quantity in electronic systems is the quasiparticle scattering rate (QPSR). A related optical scattering rate (OSR) is routinely extracted from optical data and, while it is not the same as the QPSR, it nevertheless displays many of the same features. We consider a sum rule that applies to the area under a closely related quantity, almost equal to the OSR in the low-energy region. We focus on the readjustment caused by, for example, a quasiparticle density-of-state change due to the superconducting transition. Unfortunately, no general statement about mechanism can be made solely on the energy scale in which the spectral weight readjustment in the OSR occurs.

DOI: 10.1103/PhysRevB.65.014515 PACS number(s): 74.20.Mn, 74.25.Gz, 74.72.−h

I. INTRODUCTION

A fundamental quantity in metal physics is the lifetime of the electronic excitations or quasiparticle scattering rate τ_{qp}^{-1}. This quantity can, in principle, be extracted from angle-resolved photoemission spectroscopy[1,2] (ARPES) experiments and there has been considerable recent progress, particularly in the cuprates. A related quantity is the optical scattering rate τ_{op}^{-1}, which is now routinely[3] extracted from reflectance data.[4,5] Such data is analyzed to give the real σ_1 and imaginary σ_2 part of the optical conductivity σ and $\tau_{op}^{-1}(\omega)=\Omega_p^2\ \mathrm{Re}[\sigma^{-1}(\omega)]/4\pi$, where Ω_p is the plasma frequency.[6,7] For elastic impurity scattering (characterized by a scattering time τ_{imp}), the quasiparticle scattering time is frequency ω and temperature T independent and the optical conductivity takes on its simple Drude form

$$\sigma(\omega)=\frac{\Omega_p^2}{4\pi}\left(\frac{1}{-i\omega+\tau_{op}^{-1}}\right) \tag{1}$$

with $\tau_{op}\equiv\tau_{imp}=2\tau_{qp}$. In general, inelastic scattering must also be taken into account and τ_{qp}^{-1} acquires a frequency as well as a temperature dependence. A well-studied case is the electron-phonon interaction. At finite temperature, atoms in a perfect lattice make excursions off equilibrium and this provides a scattering mechanism for the electrons. As far as quasiparticle properties are concerned, they depend only on the electron-phonon spectral density denoted by $\alpha^2F(\omega)$.[8] This function is temperature independent at low T and describes the scattering of two electrons through the exchange of a phonon. The composite function $\alpha^2F(\omega)$ is a weighted phonon-frequency distribution $F(\omega)$ seen through the electrons in which each phonon is properly weighted by its coupling to the electrons, which is provided by the electron-phonon interaction. The average coupling gives the vertex $\alpha(\omega)$. A knowledge of $\alpha^2F(\omega)$ defines the quasiparticle properties of the electrons completely and, in particular, provides us with a knowledge of the quasiparticle inverse lifetime $\tau_{qp}^{-1}(\omega,T)$ as a function of temperature and frequency. At low T and ω, specific behavior is found for $\tau_{qp}^{-1}(\omega,T)$, which can sometimes be used to characterize the nature of the electron-boson interaction involved, should it not be the electron-phonon interaction. While for phonons, τ_{qp}^{-1} varies as ω^3 in frequency and T^3 in temperature, in the marginal Fermi-liquid (MFL) model of Varma and co-workers[9,10] it varies as ω and T, respectively, and in the nearly antiferromagnetic Fermi-liquid (NAFFL) model of Pines and co-workers[11,12] it varies instead like ω^2 and T^2.

When transport properties are treated, a particular complication needs to be considered. While the quasiparticle lifetime depends only on the rate of scattering of an electron to all available final states (and equivalent scattering in terms) for transport, the momentum transfer involved in the scattering is also important since collisions with near-zero-angle (forward) scattering deplete the current much less than those that describe backward scattering. These ideas can be incorporated into a new related function $\alpha_{tr}^2F(\omega)$, which contains a vertex correction not included in $\alpha^2F(\omega)$. Even if the difference between $\alpha^2F(\omega)$ and $\alpha_{tr}^2F(\omega)$ is neglected, the optical scattering rate extracted from infrared optical data when inelastic processes are included is still not the quasiparticle scattering rate described above, although it is closely related and does contain much of the same information.

The optical scattering rate $\tau_{op}^{-1}(\omega,T)$ is extracted from reflectance data according to a well-defined procedure. The real and imaginary parts of $\sigma(\omega,T)$ are first constructed and then the real part of $\sigma^{-1}(\omega,T)$ is multiplied by the plasma frequency Ω_p squared and divided by 4π. This definition finds its motivation in a natural extension of the Drude form to

$$\sigma(\omega,T)=\frac{\Omega_p^2}{4\pi}\frac{m}{m^*(\omega,T)}\left[\frac{1}{\dfrac{1}{\tau(\omega,T)}\left\{\dfrac{m}{m^*(\omega,T)}\right\}-i\omega}\right], \tag{2}$$

which can fit any conductivity functional form. The simple Drude model results when the effective mass $m^*(\omega,T)=m$ and the scattering rate $\tau^{-1}(\omega,T)=\tau_{imp}$.

As defined $\tau_{op}^{-1}(\omega,T)$ does not obey a sum rule when an integration over frequency is performed. Recently Basov *et al.*[13] have argued, however, that a closely related quantity $\tau_{sr}^{-1}(\omega,T)$ (to be defined below) can be considered, which has the advantage of obeying a sum rule and which is closely related to $\tau_{op}^{-1}(\omega,T)$ in the low-frequency part of the spectrum. Further $\tau_{sr}^{-1}(\omega,T)$ can also be constructed from a knowledge of $\sigma(\omega,T)$ and in the cases considered by Basov *et al.*[13] is numerically almost the same as $\tau_{op}^{-1}(\omega,T)$ in the frequency range considered by them. The existence of the sum rule for $\tau_{sr}^{-1}(\omega,T)$ is used by Basov *et al.*[13] to examine the effect of the development of a superconducting gap on the scattering rate and, at higher temperatures in the underdoped regime, the development of a pseudogap. They find that in this latter case the spectral weight lost at low ω is never recovered back to the highest frequencies measured in their work, while for the superconducting gap it is. They conclude from this that the gap and pseudogap have very different microscopic origins. Here we will address the question of the validity of such a conclusion by considering in detail several microscopic models.

II. THEORY

Here we examine the sum rule obeyed by $\tau_{sr}^{-1}(\omega,T)$ and concentrate on the important issue of redistribution of spectral weight due to superconductivity, increasing temperature, and increasing scattering.

For the Drude case it is a simple matter to show that the optical scattering time is just the impurity scattering time τ_{imp} and this is twice the elastic quasiparticle lifetime

$$\tau_{op}^{-1}(\omega,T)=\frac{\Omega_p^2}{4\pi}\ \mathrm{Re}[\sigma^{-1}(\omega,T)]=\tau_{imp}^{-1}=\frac{1}{2}\tau_{qp}^{-1}, \quad (3)$$

with $\sigma(\omega,T)$ according to Eq. (1). Basov *et al.*[13] introduced a new optical lifetime denoted by $\tau_{sr}^{-1}(\omega,T)$ defined as

$$\tau_{sr}^{-1}(\omega,T)=-\frac{\Omega_p^2}{4\pi\omega}\mathrm{Im}[\epsilon^{-1}(\omega,T)], \quad (4)$$

where the dielectric function $\epsilon(\omega,T)$ is related to the optical conductivity by

$$\epsilon(\omega,T)=1+\frac{4\pi i}{\omega}\sigma(\omega,T). \quad (5)$$

The importance of $\tau_{sr}^{-1}(\omega,T)$ is that it does obey a sum rule and also that, at low energy, as we will show below, it is very nearly equal to $\tau_{op}^{-1}(\omega,T)$. Mahan has obtained[14]

$$\int_0^\infty \frac{d\omega}{\omega}\mathrm{Im}[\epsilon^{-1}(\omega,T)]=-\frac{\pi}{2}, \quad (6)$$

from which it follows that

$$\int_0^\infty d\omega\ \tau_{sr}^{-1}(\omega,T)=\frac{\pi}{2}\Omega_p^2. \quad (7)$$

Defining $\sigma'(\omega,T)=\sigma(\omega,T)/(\Omega_p^2/4\pi)$ it is easy to show that

$$\tau_{sr}^{-1}(\omega,T)=\tau_{op}^{-1}(\omega,T)\left\{1+\frac{\omega}{\Omega_p^2}\frac{1}{\sigma'^2_1(\omega,T)+\sigma'^2_2(\omega,T)}\times\left[\frac{\omega}{\Omega_p^2}-2\sigma_2'(\omega,T)\right]\right\}^{-1}. \quad (8)$$

For later reference, we have written Eq. (8) for the general case of inelastic as well as elastic scattering.

We begin with the simple case of elastic scattering only and will gain insight into the significance of the new $\tau_{sr}^{-1}(\omega,T)$ by studying this case. For the pure Drude model, σ_1' and σ_2' can be written explicitly as

$$\sigma_1'(\omega)=\frac{\tau_{imp}}{(\omega\tau_{imp})^2+1}, \quad \sigma_2'(\omega)=\frac{\omega\tau_{imp}^2}{(\omega\tau_{imp})^2+1}, \quad (9)$$

and we get after some simple algebra

$$\tau_{sr}^{-1}(\omega)=\tau_{imp}^{-1}\left\{1+\left(\frac{\omega}{\Omega_p}\right)^2\left[\frac{1}{(\Omega_p\tau_{imp})^2}+\left(\frac{\omega}{\Omega_p}\right)^2-2\right]\right\}^{-1}. \quad (10)$$

It is important to realize that while τ_{imp}^{-1} is a constant, τ_{sr}^{-1} has acquired a frequency dependence even in the Drude model. For $\Omega_p\tau_{imp}\gg 1$ and $\omega\simeq\Omega_p$ we have approximately

$$\tau_{sr}^{-1}=\tau_{imp}^{-1}(\Omega_p\tau_{imp})^2, \quad (11)$$

and τ_{sr}^{-1} has a large peak around the plasma frequency. In fact, in the limit of $\tau_{imp}^{-1}\to 0$, i.e., $\tau_{imp}\to\infty$ (vanishing impurity scattering),

$$\tau_{sr}^{-1}(\omega)=\frac{\pi}{2}\Omega_p^2\delta(\omega-\Omega_p). \quad (12)$$

This is an important result. It shows that in the clean limit the new optical scattering rate is just a δ-function peak at the plasma frequency. As impurities are introduced and a finite τ_{imp}^{-1} develops, the δ-function smears and it is the tail of this smeared δ-function at small $\omega\ll\Omega_p$ that we probe as the optical scattering rate $\tau_{op}^{-1}(\omega)$. Returning to the explicit form (10) and considering the limit $\omega/\Omega_p\ll 1$, we see

$$\tau_{sr}^{-1}(\omega)\simeq\tau_{imp}^{-1}\left[1+2\left(\frac{\omega}{\Omega_p}\right)^2\right], \quad (13)$$

so that the new and the old optical scattering rates are identical in the low-energy range and the difference between the two is only of the order $(\omega/\Omega_p)^2$. What is clear from this analysis is that the spectral weight represented by the area under the curve for $\tau_{sr}^{-1}(\omega)$ at small ω is being transferred from the δ-function at $\omega=\Omega_p$ as scattering is introduced into the system. Therefore we are dealing here with a process that is transferring spectral weight from the plasma frequency down to the frequency range $\omega\ll\Omega_p$. In particular, doubling τ_{imp}^{-1} doubles the spectral weight under $\tau_{sr}^{-1}(\omega)$ and, correspondingly, the peak at $\omega\simeq\Omega_p$ gets reduced by the appropriate amount. Its peak height drops by a factor of 4. We also note that for τ_{imp}^{-1} of the order of a few meV, the area under

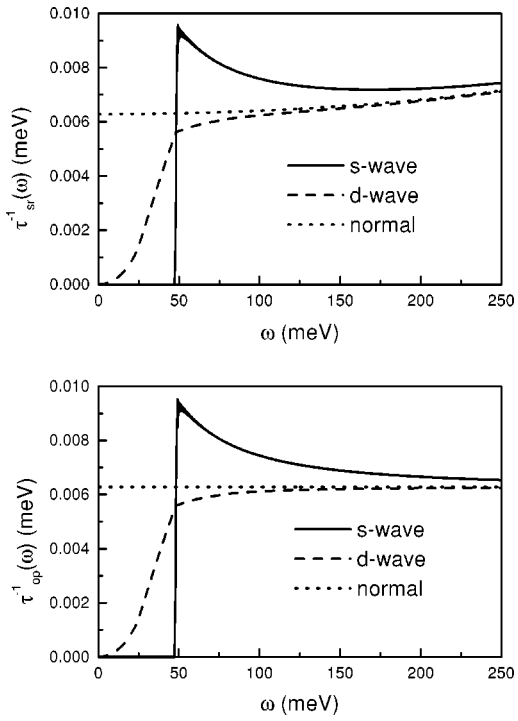

FIG. 1. A comparison of the new optical scattering rate $\tau_{sr}^{-1}(\omega)$ defined in Eq. (4) (top frame) with the conventional optical scattering rate $\tau_{op}^{-1}(\omega)$ defined by Eq. (3) (bottom frame). The dotted curves are for the normal-state Drude model with impurity (elastic) scattering only. For the conventional case $\tau_{op}^{-1}(\omega)$ is frequency independent and is equal to half the quasiparticle scattering rate and is 0.0064 meV. By contrast the new rate shows a small increase in the range to 250 meV. The solid lines are for a BCS *s*-wave superconductor and the dashed lines for a *d*-wave BCS. Both have the same impurity content as does the normal state.

$\tau_{sr}^{-1}(\omega)$ over a range of a few 100 meV is still very small (of order 10^3 meV^2) as compared to the total area under the full sum rule, which is of the order of 10^6 meV^2 for a plasma frequency $\Omega_p=1000$ meV.

III. NUMERICAL RESULTS AND DISCUSSION

In Fig. 1 we show results for $\tau_{sr}^{-1}(\omega)$ as a function of ω (dotted line, top frame) for the Drude model with $\Omega_p=1000$ meV and $\tau_{imp}^{-1}=0.0063$ meV. We see that while the new optical scattering rate increases slightly with increasing ω up to 250 meV, which is the range shown in the figure, at small frequencies it agrees well with the Drude scattering rate $\tau_{op}^{-1}(\omega)=\tau_{imp}^{-1}$ (dotted line, bottom frame), which is constant and equal to half the quasiparticle scattering rate in the normal state. A similar situation holds for the case of the superconducting state. The solid curves in the top and bottom frame apply to the *s*-wave gap with the same impurity scattering rate as was used in the Drude theory, and the dashed curve is for a two-dimensional *d*-wave superconductor with a circular Fermi surface and with a gap $\Delta(\theta)=\Delta_0\cos(2\theta)$, where Δ_0 is the gap amplitude and θ is a polar angle in the two-dimensional CuO_2 Brillouin zone. The curve in the top frame is for $\tau_{sr}^{-1}(\omega)$ and the bottom frame gives the equivalent results for $\tau_{op}^{-1}(\omega)$. The temperature is $T=10$ K. Both old and new scattering rates again agree well with each other at low ω with $\tau_{sr}^{-1}(\omega)$ showing a small deviation upwards with respect to $\tau_{op}^{-1}(\omega)$ as ω rises toward 250 meV. In the gap region, the *s*-wave case is totally different, however, from the *d*-wave case.

We discuss the *s*-wave curve first. Both old and new optical scattering rates are proportional to $\sigma_1(\omega)$, which appears in the numerator of Eqs. (3) and (4), which define the two optical scattering rates, respectively. In an *s*-wave superconductor at $T=0$ all electrons are paired and bound in a condensate. An energy Δ_0 (the gap amplitude) is therefore needed to create an excitation out of this ground state. Thus, there can be no absorption for frequencies $\omega\lesssim 2\Delta_0$ and consequently the real part of the conductivity (which is the absorptive part) is zero as are $\tau_{op}^{-1}(\omega)$ and $\tau_{sr}^{-1}(\omega)$ in this energy range. In other words, to absorb a photon, it is necessary to create a hole-particle pair. At $\omega=2\Delta_0$ there is a sharp absorption edge as shown in $\tau_{op}^{-1}(\omega)$. We see from the figure that the abrupt rise in the scattering rate overshoots its normal-state value, having a sharp maximum right at $\omega=2\Delta_0$. This sharp behavior can be traced to the singularity in the quasiparticle density-of-states $N(\varepsilon)$ as a function of energy ε. $N(\varepsilon)$ has a square-root singularity of the form $N(\varepsilon)=\mathrm{Re}\{\varepsilon/\sqrt{\varepsilon^2-\Delta_0^2}\}$, which gets reflected in $\tau_{op}^{-1}(\omega)$. Basov *et al.*[13] notice that a sum rule seems to apply for $\tau_{op}^{-1}(\omega)$ in this region of energy in the sense that the missing area below $2\Delta_0$ appears to be compensated for by the overshoot above its normal-state value in the region immediately above the gap. This sum rule, which we confirm here is, however, on a small energy scale (a few times the gap) and involves a minuscule amount of the spectral weight (of the order of 1 meV^2 in the example here) as compared to the energy scale (Ω_p) and the weight (Ω_p^2) involved in the total sum rule on $\tau_{sr}^{-1}(\omega)$. This limited "effective" sum rule applies equally well to $\tau_{op}^{-1}(\omega)$ and there is no advantage in referring to $\tau_{sr}^{-1}(\omega)$.

We turn next to the dashed curves of Fig. 1, top frame for $\tau_{sr}^{-1}(\omega)$ and bottom frame for $\tau_{op}^{-1}(\omega)$. Both apply to a *d*-wave superconductor. In this case the singularity in the quasiparticle density-of-states in the superconducting state $N(\varepsilon)$ is logarithmic, also $N(\varepsilon)$ is linear in ε at small values rather than zero; so the scattering rate, while depressed for $\omega<2\Delta_0$, is never zero except right at $\omega=0$. It is clear from the figure that this weaker singularity does not lead to an overshoot above the Drude scattering rate just beyond $\omega=2\Delta_0$. Instead, the normal state is approached from below, and even in $\tau_{sr}^{-1}(\omega)$ up to 250 meV, the normal and the superconducting curves have not yet come to cross so that the readjustment of spectral weight in $\tau_{op}^{-1}(\omega)$ due to the superconducting transition is spread over a very large frequency range at fixed plasma frequency. Of course one can conceive of processes that would also result in a change in plasma frequency, but such a possibility goes beyond the scope of this work. We do not wish, for example, to consider multiband effects.

So far we have looked only at elastic impurity scattering.

It is of interest to also consider the inelastic case. To be specific, we start with the electron-phonon interaction for which the required information on the coupling between electrons and phonons is completely captured in the spectral function $\alpha^2F(\omega)$. For this case the normal-state conductivity takes on a particularly simple form because of the existence of Migdal's theorem, which allows us to neglect vertex corrections. If, for simplicity, we also neglect the differences between $\alpha^2F(\omega)$ and the equivalent transport[15,16] $\alpha^2_{tr}F(\omega)$,

$$\sigma(\omega)=\frac{\Omega_p^2}{4\pi}\int_0^{\omega}d\nu\frac{1}{\omega+\tau_{imp}^{-1}-\Sigma(\nu)-\Sigma(\nu-\omega)}, \quad (14)$$

where $\Sigma(\omega)$ is the self-energy of the electrons brought about by their coupling to the phonons. At zero temperature it is given by

$$\Sigma(\omega)=\int_0^{\infty}d\Omega\,\alpha^2F(\Omega)\ln\left|\frac{\Omega-\omega}{\Omega+\omega}\right|-i\pi\int_0^{|\omega|}d\Omega\,\alpha^2F(\Omega). \quad (15)$$

More generally, the imaginary part of the self-energy $[-2\Sigma_2(\omega)]$ gives a quasiparticle scattering rate, which is temperature and frequency dependent. The previously stated result that it varies as ω^3 is easily verified from Eq. (15) and follows directly from a Debye model with $\alpha^2F(\Omega)\propto\Omega^2$. Further, the NAFFL model[11,12] corresponds to a small omega dependence for the spectral density, which is linear while for the MFL model[9,10] it is constant. It is also clear from Eq. (14) that for $\Sigma(\omega)=0$ we recover the simple Drude theory, which includes only impurity scattering.

Results for the optical scattering rate in an electron-phonon system are given in Fig. 2. The top frame gives results in the limited frequency range up to 500 meV while the bottom frame shows results up to 2000 meV. The plasma frequency has been set to 1000 meV. There are two sets of two curves. The solid and dash-dotted lines form a pair and apply to $\tau_{op}^{-1}(\omega)$ and $\tau_{sr}^{-1}(\omega)$, respectively, for impurity scattering only and are given for comparison. The other pair, dashed and dotted lines, respectively, include in addition to impurity scattering some inelastic electron-phonon contribution. The spectrum used for $\alpha^2F(\omega)$ was that utilized for BaKBiO,[17] a superconductor with a T_c of 29 K. This is for illustration purposes only, as there is strong evidence that BaKBiO is not a conventional electron-phonon superconductor.[18,19] Here we show results at $T=10$ K in the normal state. For more details of the spectrum the reader is referred to the review by Marsiglio and Carbotte.[17] Up to roughly 75 meV, old and new scattering rates deviate very little from each other as commented on before. Also, both sets of two curves start from the same point at $\omega=0$ where only the elastic scattering contributes. As ω increases towards 500 meV (top frame) the Drude case remains almost constant (exactly constant for the solid curve) while the other two curves, which include inelastic scattering, grow considerably. The dashed curve, which gives $\tau_{op}^{-1}(\omega)$, shows saturated behavior for frequencies exceeding about 100 meV. This is typical of an electron-phonon system and corresponds to the saturated value of the underlying quasiparticle scattering rate. It is clear from formula (15) that the imaginary part of $\Sigma(\omega)$ takes on its saturated value when $|\omega|$ in the last integral equals the maximum phonon energy in $\alpha^2F(\omega)$ (corresponding to ω_D—the Debye energy—for a Debye spectrum). Beyond this value of $|\omega|$, increasing the upper limit in the integral leaves its value unchanged. The dotted curve, however, which applies to $\tau_{sr}^{-1}(\omega)$, does not saturate at all. In fact, it displays a rather rapid rate of increase around 500 meV in the top frame of Fig. 2. This is expected since, as we have already described and stress again, the new $\tau_{sr}^{-1}(\omega)$ has a very large peak at the plasma frequency. Details are given in the bottom frame of Fig. 2. The quantities and labels are the same as in the top frame but now a larger range of frequency is shown, up to 2000 meV—twice the plasma frequency. The very large δ-function-like peak for the case when only elastic scattering is present is clearly seen at 1000 meV (dash-dotted curve).[20] In the corresponding dotted curve, which additionally includes inelastic scattering, the peak has been further broadened (by about 100 meV), but the peak height is still very large compared to the value of the corresponding scattering rates in the infrared region below a few hundred meV. Note also, and we need to stress this, that the usual optical scattering rates, solid curve for the Drude (pure elastic case) and dashed curve for the electron-

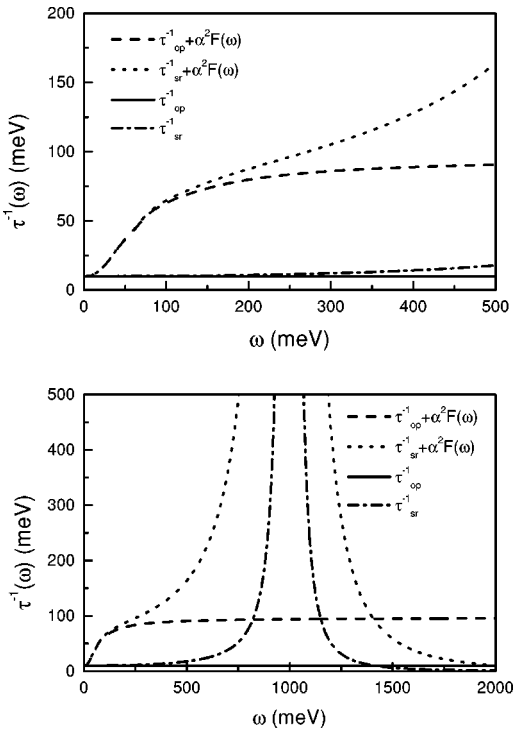

FIG. 2. Top frame compares conventional and new optical scattering rates for (a) elastic scattering only (solid and dash-dotted curves, respectively) and (b) with inelastic scattering also included (dashed and dotted curves, respectively). The model for inelastic scattering is the electron-phonon interaction previously considered for BaKBiO, a superconductor with a $T_c=29$ K. All curves are in the normal state. The frequency range is limited to 500 meV in the top frame. The bottom frame extends the range to 2000 meV, twice the plasma frequency in our model. The new scattering rates display a very large peak at $\Omega_p=1000$ meV.

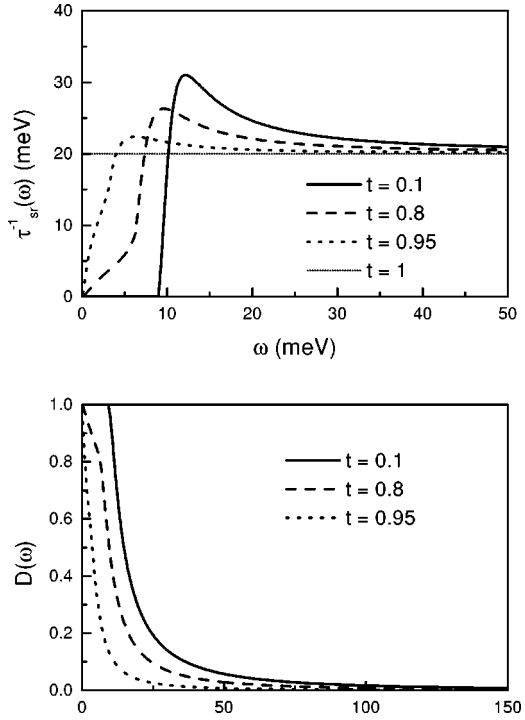

FIG. 3. The top frame shows the new optical scattering rate $\tau_{sr}^{-1}(\omega)$ vs ω in the range up to 50 meV. The dotted line is the normal state and is for reference. The other curves are for a BCS *s*-wave superconductor at three temperatures, $t=T/T_c=0.95$, 0.8, and 0.1. We see readjustment of spectral weight in $\tau_{sr}^{-1}(\omega)$ as a result of the superconducting transition. The bottom frame gives $D(\omega)$ as defined in Eq. (16) vs ω at $t=T/T_c=0.95$ (dotted curve), 0.8 (dashed curve), and 0.1 (solid curve). The upper limit ν ranges up to 150 meV.

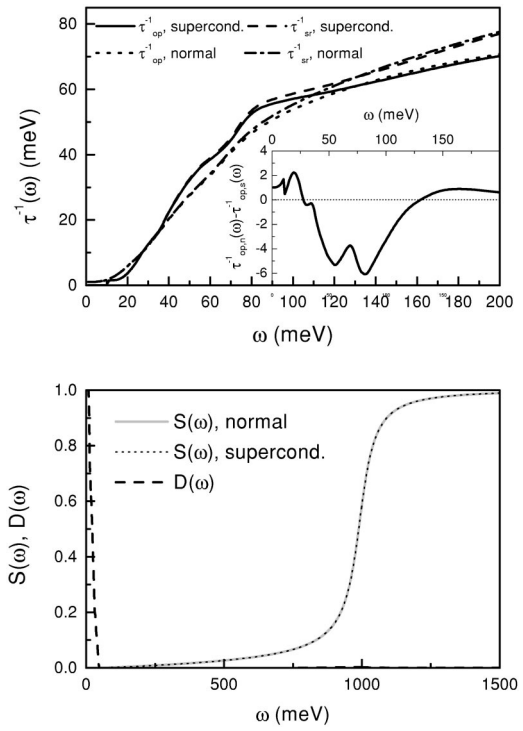

FIG. 4. Top frame shows the optical scattering rate for a model electron-phonon spectrum for BaKBiO including an impurity scattering rate of 1 meV. The temperature is $T/T_c=0.2$ with $T_c=29$ K and the plasma frequency was taken to be 1000 meV for illustration purposes. The solid curve is the conventional $\tau_{op}^{-1}(\omega)$ in the superconducting state to be compared with the short dashed curve in the normal state. The dashed curve is the new scattering rate [Eq. (4)] (superconducting state) with the dash-dotted curve in the normal state. The inset gives $\tau_{op,n}^{-1}-\tau_{op,s}^{-1}$ vs ω. The bottom frame gives $D(\omega)$ according to Eq. (16) and the gray solid and the dotted line give $S(\omega)=\int_0^{\omega}d\nu\,\tau_{sr,s(n)}^{-1}(\nu)/\int_0^{\infty}d\nu\,\tau_{sr,n}^{-1}(\nu)$.

phonon case, show no equivalent peak and in fact saturate rapidly in the energy range considered in this figure.

We return to the BCS *s*-wave superconducting state. In Fig. 3, top frame, we show results for $\tau_{sr}^{-1}(\omega)$ vs ω in the superconducting state at three reduced temperatures $T/T_c=0.1$ (solid), 0.8 (dashed), and 0.95 (dotted). The normal state (fine dots) with $\tau_{imp}^{-1}=20$ meV (the same impurity scattering as in all other curves) is also shown for comparison. This larger value of τ_{imp}^{-1}, compared with that used in Fig. 1, increases the amount of spectral weight lost below the gap in the superconducting case, but this area is still very small as compared with the total spectral weight involved in the sum rule. In the lower frame we give more details on the readjustment of the $\tau_{sr}^{-1}(\omega)$ brought about by the transition. We define a normalized difference in spectral weight as a function of increasing frequency ν. Here $\tau_{sr,n}^{-1}(\omega)$ and $\tau_{sr,s}^{-1}(\omega)$ stand for normal and superconducting, state respectively,

$$D(\nu)=\frac{\int_0^{\nu}d\omega[\,\tau_{sr,n}^{-1}(\omega)-\tau_{sr,s}^{-1}(\omega)\,]}{\int_0^{\nu}d\omega\,\tau_{sr,n}^{-1}(\omega)}. \tag{16}$$

The solid curve applies to $T/T_c=0.1$, the dashed to 0.8, and the dotted to 0.95 with a plasma frequency of 1000 meV and $\tau_{imp}^{-1}=20$ meV. We see that in all cases the readjustment is quite complete by 50 meV, which is about five times $2\Delta_0$. Of course, the higher the temperature, the faster $D(\nu)$ falls towards zero. It is clear that the scale of readjustment in scattering-rate spectral weight is of the order of a few times the gap. In the above we have used $\tau_{sr}^{-1}(\omega)$ but we could equally well have used $\tau_{op}^{-1}(\omega)$. The overall sum rule on $\tau_{sr}^{-1}(\omega)$ is already satisfied at a sufficiently low frequency such that the two scattering rates are still nearly equal.

We continue with the electron-phonon interaction and consider the superconducting state with *s*-wave gap symmetry for a reasonably clean sample with $\tau_{imp}^{-1}=1.0$ meV for the elastic impurity scattering, as shown in Fig. 4. At zero temperature and zero frequency the scattering rate approaches 1 meV in the normal state. For any nonzero ω, additional scattering takes place due to the inelastic processes. Also at any finite temperature some phonons will always be excited and consequently there will also be a finite $\omega=0$ intercept to $\tau_{op}^{-1}(\omega)$ even if τ_{imp}^{-1} is zero. In Fig. 4, top frame, we show two sets of two curves, which serve to illustrate our main points. The solid and dashed curves are in the superconducting state for $\tau_{op}^{-1}(\omega)$ and $\tau_{sr}^{-1}(\omega)$, respectively,

while the dotted and dash-dotted curves are the corresponding set for the normal state. At the highest frequency shown (200 meV) the curves for $\tau_{sr}^{-1}(\omega)$ already show the clear deviation upward when compared with those for $\tau_{op}^{-1}(\omega)$. Here we wish to stress the low-energy region. The superconducting gap is clearly seen in the curves for the superconducting state below 10 meV and some spectral weight is lost when compared with the normal state, but this suppression is small when contrasted with the BCS case described in Fig. 3. The absorption edge at $2\Delta_0$ is now not as sharp and does not immediately overshoot the normal curve and there is no peak. In fact, it is not until approximately 30 meV that the superconducting curves first cross the normal-state curves. As compared with the simple *s*-wave BCS case of Figs. 1 and 3, the spectral weight readjustment in the pure limit with the inelastic-scattering case is occurring over a much larger energy region [see Eq. (6)]. We note that this is so even though the corresponding density of quasiparticle states remains singular at Δ_0 for an electron-phonon superconductor, yet this hardly shows up in the corresponding scattering rate.

In the bottom frame of Fig. 4 we show results for the difference $D(\nu)$ function (dashed curve) defined in Eq. (16) and for the sum rule normalized to unity (gray solid curve for the normal and dotted curve for the superconducting state). It is clear from the dashed curve that some readjustment in spectral weight takes place over quite a large energy scale. The insert in the top frame gives a clearer indication of this fact. What is plotted is the difference $\tau_{op,n}^{-1}(\omega)-\tau_{op,s}^{-1}(\omega)$ as a function of ω. This difference remains positive until about 30 meV (approximately six times the gap) after which it displays a compensating negative region, which more than cancels out the lost spectral weight below 30 meV. Beyond 120 meV it becomes slightly positive again. The local minima and maxima in the difference function are related to the minima and maxima in the phonon spectrum, which sets the scale for this structure. Clearly, no general statement about the appropriate frequency range over which the readjustment occurs can be made. It depends on such details as coupling strength, the size of the maximum boson energy in $\alpha^2F(\omega)$, and the elastic impurity scattering rate. Finally note the rapid rise in the sum-rule integral (gray solid curve for the normal and black dotted curve for the superconducting state) as we integrate through the plasma energy. This curve serves to show that for the BaKBiO spectrum used here to discuss the inelastic scattering, the entire region up to $\lesssim$500 meV makes only a relatively small contribution to the total sum rule so that the spectral readjustments described are very small indeed in comparison.

We repeat the results of Fig. 4 in Fig. 5 with $\tau_{imp}^{-1}=25.0$ meV, which is closer to the dirty limit. Here there is a clear sign of the density-of-states singularity at Δ_0. Much more spectral weight is shuffled to and fro at low frequencies; otherwise the two cases are similar.

We have already given an example of a BCS *d*-wave, which showed no clear readjustment in scattering-rate spectral weight corresponding to the density-of-states change in the region of a few times the gap. The calculations were done for Born (weak) scattering. The situation is quite different in the case of unitary (strong) scattering. For details on the various impurity models the reader is referred to earlier literature.[21] Here it is sufficient to state that for the unitary case a *T*-matrix approach is used to describe the impurity scattering (strong scattering) instead of lowest-order perturbation theory for the Born case (weak scattering). In Fig. 6 we show results for $\tau_{op}^{-1}(\omega)$ for a BCS *d*-wave superconductor with $\Delta_0=24$ meV and elastic-scattering strength $t^+=1/(2\pi\tau_{imp})=0.2$ meV. The dotted line is for comparison

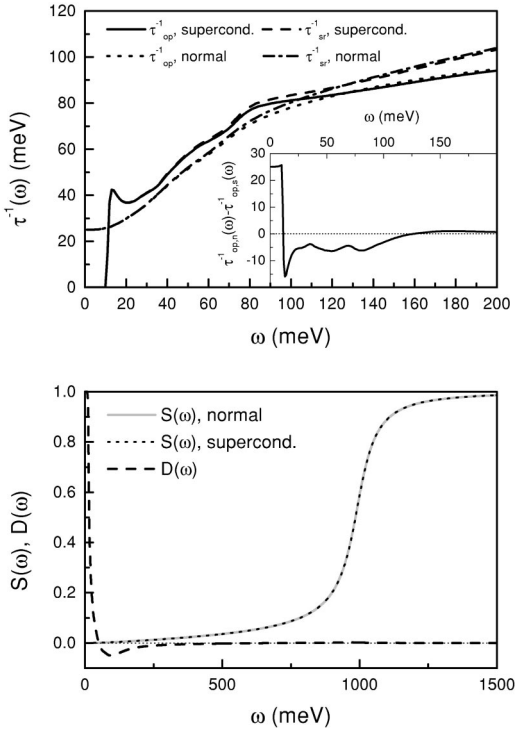

FIG. 5. Same as for Fig. 4, but for an impurity scattering rate of 25 meV.

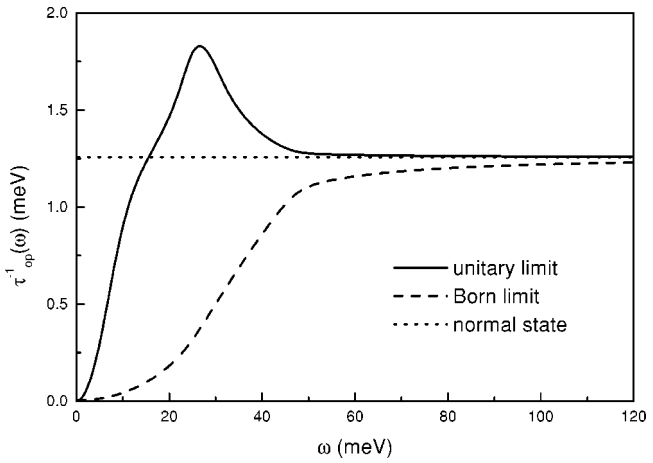

FIG. 6. The new optical scattering rate $\tau_{sr}^{-1}(\omega)$ defined in Eq. (4) for a *d*-wave BCS superconductor with its normal-state counterpart (dotted curve). The impurity scattering is 1.25 meV. The dashed curve is for Born approximation while the solid curve is for the unitary limit. This latter curve reflects the underlying quasiparticle density of states and peaks at the gap.

and is in the normal state and the dashed line is for the superconducting state with impurity scattering in the weak-scattering limit (Born approximation). In sharp contrast to the Born approximation, for unitary scattering (solid curve) we see in $\tau_{op}^{-1}(\omega)$ a recognizable although somewhat distorted picture of the density of states. While spectral weight is lost below approximately 20 meV it is largely regained above 20 meV in a region of frequencies, of a few times the gap. It is clear from these results that impurity scattering plays an important role in determining the redistribution of spectral weight in $\tau_{op}^{-1}(\omega)$ on entering the superconducting state.

Finally, we present results for the *d*-wave case, which includes inelastic scattering. They are presented in our last figure and are based on generalized Eliashberg equations[6,7] previously used by us to discuss the optical conductivity in the high-T_c cuprates. We will not give mathematical details of the computations here but refer the reader to the literature.[22–24] A summary is as follows: it is possible to understand the measured in-plane infrared properties of the CuO_2 plane in terms of generalized Eliashberg equations, which explicitly include *d*-wave symmetry in the gap channel. The inelastic scattering, which enters both gap and renormalization channels is modeled through an electron-boson spectral density $I^2\chi(\omega)$ closely related to the electron-phonon spectral density $\alpha^2F(\omega)$ introduced and discussed earlier. For the oxides, the microscopic origin of $I^2\chi(\omega)$ is not the electron-phonon interaction. In the NAFFL model of Pines and co-workers[11,12] it is the exchange of spin fluctuations between the charge carriers which leads to pairing in the $d_{x^2-y^2}$ channel. In the MFL model of Varma and co-workers[9,10] the fluctuation spectrum has both charge and spin contributions. Both the above models are phenomenological, however, and in our previous work we have used a fit to optical data to fix $I^2\chi(\omega)$. Such a procedure has been very successful[15,16,22–24] in revealing special features of the spectral density $I^2\chi(\omega)$. Among these features is the long tail in $I^2\chi(\omega)$ extending to 400 meV (the cutoff in our numerical work) which is characteristic of the NAFFL model and also of the MFL model of Varma and co-workers[9,10] Another feature is the observation of the growth of the 41-meV spin resonance observed in neutron scattering[25] and now seen as well in the optics and in ARPES.

In Fig. 7 (top frame) we show results for the case of optimally doped $Tl_2Sr_2CuO_{6+\delta}$ (Tl2201).[24] What is shown is $\tau_{op}^{-1}(\omega)$ in meV vs ω up to 250 meV. There is no significant difference between $\tau_{op}^{-1}(\omega)$ and $\tau_{sr}^{-1}(\omega)$ in this energy range as first noted by Basov *et al.*[13] Our normal-state results at $T=300$ K (dashed curve) are based on a model for the spin-fluctuation spectrum $I^2\chi(\omega)$ first introduced by Pines and co-workers:[11,12]

$$I^2\chi(\omega)=I^2\frac{\omega/\omega_{SF}}{1+(\omega/\omega_{SF})^2}, \tag{17}$$

(referred to as MMP), where I^2 is the coupling between the charge carriers and spin fluctuations, which are taken to have a characteristic energy ω_{SF}. Both parameters are determined

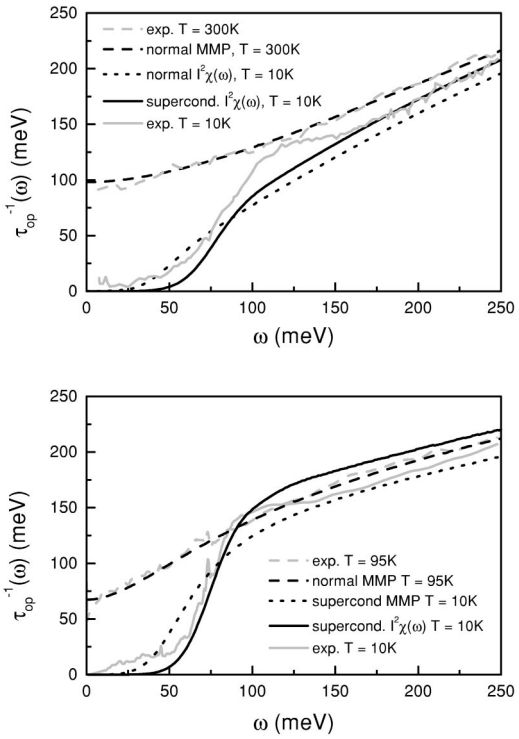

FIG. 7. Top frame gives results of theoretical calculations for $\tau_{sr}^{-1}(\omega)$ vs ω for Tl2201. The dashed curve is for the normal state at $T=300$ K. The solid curve is in the superconducting state at $T=10$ K to be compared with the dotted curve (normal state at the same temperature). For the model electron-boson spectral density $I^2\chi(\omega)$ used, refer to the text. The experimental data is from Puchkov *et al.* (Ref. 4), the dashed gray curve at 300 K and the solid gray curve at 10 K. The bottom frame gives similar results for twinned, optimally doped YBCO. The experimental data is from Basov *et al.* (Ref. 13), the dashed gray curve at 95 K and the solid gray curve at 10 K. The other three curves are results of theoretical calculations. The solid curve is based on a model for the electron-spin fluctuation spectral density $I^2\chi(\omega)$ which included the 41-meV spin resonance seen in inelastic neutron scattering and represents the superconducting state at $T=10$ K to be compared with the dotted curve [MMP model (Refs. 11 and 12) at the same temperature]. The dashed curve is based on the same MMP model and represents the normal-state scattering rate at $T=95$ K.

to get a best fit to the real part of the infrared conductivity at $T=300$ K. We find $\omega_{SF}=100$ meV. Our superconducting state results at $T=10$ K (solid line) are based on a modification of the MMP model in which we have added a spin-resonance peak at $\omega_r=35$ meV.[24] It is noted that for superconducting-state calculations a set of two coupled Eliashberg equations are solved, each containing a spectral density $I^2\chi(\omega)$. This function need not be the same in renormalization (which determines the normal-state properties) and gap channels. We introduce a constant factor g to account roughly for any such difference in the gap channel. The new parameter g is then fixed to get the measured value of T_c; here $g=0.82$. It should be pointed out that this coupling to a spin resonance was derived from optical data and has not yet been observed in other experiments. We also included, for comparison, normal-state results at $T=10$ K

(dotted line) for the same $I^2\chi(\omega)$. This last result is not accessible to experiment. The two gray curves represent experimental data by Puchkov *et al.*;[4] dashed gray is for $T=300$ K and solid gray is for $T=10$ K. It is clear from the figure that the superconducting curve is always below the 300 K normal-state data and the energy scale for the readjustment of spectral weight between the two cases is many times the gap. On the other hand, if one refers the 10-K superconducting state (solid curve) result to the 10-K normal-state result (dotted curve), the weight lost in the region below ~ 85 meV is more than made up for in the region above the crossover and extending to 250 meV. Also some readjustment is still occurring well beyond this energy scale. Of course, the experimentalist in his analysis can only compare between the normal-state data (above T_c) and the data in the superconducting state.

We make a final point in Fig. 7, bottom frame. We show results for $\tau_{op}^{-1}(\omega)$ in the case of a twinned $YBa_2Cu_3O_{6.95}$ (YBCO) single crystal. The gray curves show experimental results for $\tau_{op}^{-1}(\omega)$ obtained by Basov *et al.*[26] on a twinned sample in the normal state at 95 K (dashed gray curve) and in the superconducting state at 10 K (gray solid curve). For comparison we show two sets of theoretical results based on an Eliashberg *d*-wave formalism and two different models for the electron-boson exchange spectral density $I^2\chi(\omega)$. For the solid curve we use the $I^2\chi(\omega)$ result of Schachinger *et al.*,[27] which includes the 41-meV spin resonance seen in inelastic spin-polarized neutron experiments and also in the optical data. For the dotted curve we use instead a MMP spectrum with $\omega_{SF}=20$ meV, which represents a scale for the spin fluctuations and which gives a best fit to the normal state $\sigma_n(\omega)$ (dashed curve). An overall cutoff of 400 meV is applied to $I^2\chi(\omega)$ for the Eliashberg calculations, along with $g=0.98$ to get the measured $T_c=92.4$ K. The important point we wish to make about these two theoretical results for the superconducting state is that they differ only in the shape of the assumed underlying spectral density $I^2\chi(\omega)$. In particular, both give very similar results for the electronic density-of-states $N(\varepsilon)$ in the superconducting state. Yet they differ considerably when used to consider spectral redistribution on entering the superconducting state. As compared with the normal-state curve (gray, experimental data) more spectral weight is lost at low ω in the solid than in the dotted curve. Much of the loss is made up at higher energies in the solid curve while the dotted curve never crosses the experimental normal-state curve in the energy range considered in this figure. It is clear that for inelastic scattering, changes in shape of the underlying spectral density $I^2\chi(\omega)$ can importantly influence the resulting spectral-weight shifts observed in the scattering rate when the material becomes superconducting. These changes are additional to any accompanying density-of-state changes that may also be present. It is the growth of the spin-resonance peak, which is present in the superconducting state and not in the normal state for optimally doped systems that is responsible for the overshoot of the solid curve above the dashed curve (normal state) in our calculations. In underdoped systems the spin resonance starts at the pseudogap temperature.

IV. SUMMARY

Sum rules on optical quantities can be a powerful tool in making pertinent inferences from data and have played an important role in the analysis of such data. Reflectance data is routinely analyzed to obtain the real and imaginary parts of the conductivity, and, guided by the structure of the generalized Drude form for the conductivity, a frequency- and temperature-dependent optical scattering rate $\tau_{op}^{-1}(\omega)$ can be constructed from a knowledge of the conductivity. This optical scattering rate is not the quasiparticle scattering rate at the Fermi surface but is rather some complicated average over frequency and over the Fermi surface (should there be anisotropy, a complication we have not treated here). Nevertheless, the two rates are closely connected and valuable information about electron scattering and inelastic processes is obtained from a knowledge of $\tau_{op}^{-1}(\omega)$. No sum rule applies to the integral under the curve $\tau_{op}^{-1}(\omega)$.[28] It is possible, however, to define a related quantity, which also has units of energy; this new scattering rate, denoted $\tau_{sr}^{-1}(\omega)$, does satisfy a sum rule. It also has the remarkable property that in the low-energy region of the infrared spectrum, it is numerically equal to the optical scattering rate $\tau_{op}^{-1}(\omega)$. For a simple Drude model in the normal state with only impurity (elastic) scattering and for which $\tau_{op}^{-1}(\omega)$ is a constant independent of frequency and equal to half the quasiparticle scattering rate, $\tau_{sr}^{-1}(\omega)$ differs from $\tau_{op}^{-1}(\omega)$ only by a term of order $(\omega/\Omega_p)^2$.

Some insight into the physical meaning of the sum rule on $\tau_{sr}^{-1}(\omega)$ is obtained from the observation that in a simple Drude model for the normal state and in the limit of zero elastic scattering, $\tau_{sr}^{-1}(\omega)$ becomes a δ-function at the plasma frequency. As impurity scattering is introduced (by impurity doping, for example), the δ-function at Ω_p broadens by an amount related to the value of the impurity scattering rate τ_{imp}^{-1}. This means that as τ_{imp}^{-1} is increased, the spectral weight at small ω has been transferred to this region from the plasma frequency, so that the readjustment of spectral weight in $\tau_{sr}^{-1}(\omega)$, brought about by an increase in elastic scattering is over the entire frequency range up to Ω_p. When inelastic scattering, is included, the same effect takes place (to be specific we have considered the case of an electron-phonon system). The peak at Ω_p in $\tau_{sr}^{-1}(\omega)$ is broader than in Drude theory and an increase in the strength of the electron-phonon interaction again results in the transfer of weight from the plasma frequency to the low-ω region. Of course, as the coupling is further increased, the amount of spectral weight in $\tau_{sr}^{-1}(\omega)$, which resides at low energies, say within one quarter of the plasma frequency, could become a substantial fraction of that left in the peak around Ω_p. In this case the low-ω region is more representative of the total spectral weight available under the $\tau_{sr}^{-1}(\omega)$ vs ω curve.

We have examined several specific cases in some detail. For a BCS *s*-wave superconductor with only elastic scattering we find that the missing spectral weight from below twice the gap Δ_0 [where $\tau_{sr}^{-1}(\omega)$ is zero] is largely compensated for in the region immediately above the gap where $\tau_{sr}^{-1}(\omega)$ shows a peak that is a reflection of the density of

electronic states in the superconductor. This last quantity has a square-root singularity at $\omega=\Delta_0$. In this example readjustment of the spectral weight is occurring only at low energies ($\omega \ll \Omega_p$) and the amount involved is very small compared to the total sum. Therefore we are dealing here with an effective sum rule, operative over a limited energy region.

For a *d*-wave superconductor with impurity scattering treated in the Born approximation, the situation is completely different. A depression in $\tau_{sr}^{-1}(\omega)$ over its value in the normal state is observed in the region below the gap with no compensating spectral weight gained immediately above the gap. In fact, the depression in $\tau_{sr}^{-1}(\omega)$ persists to very large energies as compared with Δ_0 and the superconducting curve is not observed to cross the normal curve below 250 meV and never crosses in our calculations to the highest energy checked ($2\Omega_p$). In $\tau_{sr}^{-1}(\omega)$ the readjustment in spectral weight due to the onset of superconductivity is spread over the entire region.

Another interesting case is *s*-wave-gap symmetry with inelastic scattering due, for example, to the electron-phonon interaction. For the clean limit we find that the spectral-weight readjustment in $\tau_{sr}^{-1}(\omega)$ due to the onset of superconductivity when compared with the normal state is spread over a very large frequency range very much like in the *d*-wave BCS case and quite different from the BCS *s*-wave case. It is certainly not confined to the region of a few times the gap. Even though the electronic density-of-states has the same singularity at $\omega=\Delta_0$ as in the BCS case, no peak is seen just above $2\Delta_0$. Note that in this example the same microscopic mechanism as in BCS is operative, yet the net results are quite different. Readjustments due to $N(\varepsilon)$ are not seen directly in the clean limit. To see them, impurity scattering is required. This applies equally well, in a slightly modified form, to the *d*-wave case. For pure elastic scattering, spectral-weight readjustment takes place over the entire range of the plasma frequency, but including some impurity scattering in the unitary limit changes $\tau_{op}^{-1}(\omega)$ radically in the gap region. In this instance, the loss of spectral weight below the gap is seen to be largely compensated for by an overshoot around the gap (not twice the gap).

There is one further complication; in highly correlated systems the underlying spectral density in boson-exchange formulations has its microscopic origin in electronic correlations and is therefore expected to show changes as the electronic system changes phase. These changes in charge-carrier-fluctuation spectral density can induce scattering-rate spectral changes, which are similar to those due to electronic density-of-states readjustments and it is then difficult to separate the two effects.

It is clear from these examples that no general statement can be made about spectral-weight readjustment in the scattering rate due to microscopic changes in the underlying system. It is apparent that in addition to the gap-energy scale, the frequency scale of the source of the inelastic scattering influences the frequency range of spectral-weight readjustment in this sum rule—the higher this scale, the higher the frequency affected. We conclude that it is not possible to make firm conclusions about the mechanism on the basis of the magnitude of the energy scale on which readjustment of spectral weight in the optical scattering rate is taking place.

ACKNOWLEDGMENTS

We thank D. N. Basov for introducing us to this issue. This research was supported by the Natural Sciences and Engineering Research Counsel of Canada (NSERC) and by the Canadian Institute for Advanced Research (CIAR).

[1] T. Valla, A.V. Fedorov, P.D. Johnson, B.D. Wells, S.L. Hulbert, G. Li, G.D. Ju, and N. Koshizuka, Science **285**, 2110 (1999).

[2] A. Kamenski, A.J. Mesot, H. Fretwell, J.C. Campuzano, M.R. Norman, M. Randerias, H. Ding, T. Sato, T. Takahashi, T. Mochidu, K. Kadowaki, and H. Hoechst, Phys. Rev. Lett. **84**, 1788 (2000).

[3] T. Timusk and D. B. Tanner, in *Physical Properties of High Temperature Superconductors*, edited by D. M. Ginsberg (World Scientific, Singapore, 1989), Vol. I, p. 339; Vol. III, p. 363.

[4] A. Puchkov, D.N. Basov, and T. Timusk, J. Phys.: Condens. Matter **8**, 10 049 (1996).

[5] C.C. Homes, T. Timusk, R. Liang, D.A. Bonn, and W.N. Hardy, Phys. Rev. Lett. **71**, 1645 (1993).

[6] E. Schachinger, J.P. Carbotte, and F. Marsiglio, Phys. Rev. B **56**, 2738 (1997).

[7] E. Schachinger and J.P. Carbotte, Phys. Rev. B **57**, 13 337 (1998).

[8] J.P. Carbotte, Rev. Mod. Phys. **62**, 1027 (1990).

[9] C.M. Varma, P.B. Littlewood, S. Schmitt-Rink, E. Abrahams, and A.E. Ruckenstein, Phys. Rev. Lett. **63**, 1996 (1989); **69**, 497 (1990).

[10] E. Abrahams and C.M. Varma, cond-mat/0003135 (unpublished).

[11] A.J. Millis, H. Monien, and D. Pines, Phys. Rev. B **42**, 167 (1990).

[12] P. Monthoux and D. Pines, Phys. Rev. B **47**, 6069 (1993).

[13] D.N. Basov, E.J. Singley, and S.V. Dordevic, cond-mat/0103507 (unpublished).

[14] G. D. Mahan, *Many-Particle Physics* (Plenum, New York, 1981).

[15] F. Marsiglio, T. Startseva, and J.P. Carbotte, Phys. Lett. A **245**, 172 (1998).

[16] F. Marsiglio, J. Supercond. **12**, 163 (1999).

[17] F. Marsiglio and J.P. Carbotte, Aust. J. Phys. **50**, 975 (1997). Note that while we used this spectrum for calculations in this paper, our conclusion was that the conventional electron-phonon mechanism does not explain superconductivity in this material.

[18] A.V. Puchkov, T. Timusk, W.D. Mosley, and R.N. Shelton, Phys. Rev. B **50**, 4144 (1994); A.V. Puchkov, T. Timusk, M.A. Karlow, S.L. Cooper, D.D. Han, and D.A. Payne, *ibid.* **52**, 9855 (1995).

[19] F. Marsiglio, J.P. Carbotte, A. Puchkov, and T. Timusk, Phys. Rev. B **53**, 9433 (1996).

[20] Note that with the vertical scale used, the curve actually does not look like a δ-function. However, the dot-dashed curve has a maximum at $\approx 10^6$ meV. If this scale were used, the curve

would indeed look like a δ-function.

[21] I. Schürrer, E. Schachinger, and J.P. Carbotte, Physica C **303**, 287 (1998).

[22] J.P. Carbotte, E. Schachinger, and D.N. Basov, Nature (London) **401**, 354 (1999).

[23] E. Schachinger and J.P. Carbotte, Phys. Rev. B **62**, 9054 (2000).

[24] E. Schachinger and J.P. Carbotte, Physica C **341-348**, 79 (2000).

[25] Ph. Bourges, Y. Sidis, H.F. Fong, B. Keimer, L.P. Regnault, J. Bossy, A.S. Ivanov, D.L. Milius, and I.A. Aksay, in *High Temperature Superconductivity*, edited by S. E. Barnes *et al.*, AIP Conf. Proc. No. **483** (AIP, Woodbury, NY, 1999), pp. 207–212.

[26] D.N. Basov, A.V. Puchkov, R.A. Hughes, T. Strach, J. Preston, T. Timusk, D.A. Bonn, R. Liang, and W.H. Hardy, Phys. Rev. B **49**, 12 165 (1994).

[27] E. Schachinger, J.P. Carbotte, and D.N. Basov, Europhys. Lett. **54**, 380 (2001).

[28] See, however, N. Shah and A.J. Millis, cond-mat/0104502 (unpublished) for a potentially useful identity involving this integral.